Microfluidics Nanofluidics manuscript No.
(will be inserted by the editor)

Reliable addition of reagents into microfluidic droplets

Jayaprakash Sivasamy · Yong Cai Chim · Teck-Neng Wong · Nam-Trung Nguyen · Levent Yobas

Received: date / Revised version: date

Abstract This paper reports a design that reliably adds reagents into droplets by exploiting the physics of fluid flow at a T-junction in the microchannel. An expanded section right after the T-junction enhances merging of a stream with a droplet, eliminates the drawbacks such as extra droplet formation and long mixing time. The expanded section reduces the pressure build-up at the T-junction and minimizes the tendency to form extra droplets; plays the role in creating low Laplace pressure jump across the interface of the droplet forming from the T-junction which reduces the probability of forming extra droplet in the merging process; provides space for droplet coalescence if there is an extra droplet due to droplet break-up before merging. In this design, after merging, the reactants are in axial arrangement

Jayaprakash Sivasamy · Yong Cai Chim · Teck-Neng Wong

E-mail: mtnwong@ntu.edu.sg · Nam-Trung Nguyen

School of Mechanical and Aerospace Engineering, Nanyang Technological University, 50 Nanyang Avenue, Singapore 639798, Singapore

Jayaprakash Sivasamy · Levent Yobas

Institute of Microelectronics, A*STAR (Agency for Science, Technology and Research), 11 Science Park Road, Singapore Science Park II, Singapore 117685.

inside the droplets which leads to faster mixing. Reliable addition of reagent to the droplets happens for the combination of flow rates in a broad range from 25 μl/hr to 250 μl/hr, for both DI water (Q_{DI}) and fluorescent (Q_{fluo}) streams.

Keywords Droplet Microfludics · Droplet Merging · Reagent addition · Droplet Coalescence

1 Introduction

Microfluidic systems developed with multiphase flows are used for miniaturizing chemical and biological laboratory techniques [1,2]. Microscale multiphase flows such as aqueous droplets in oil are useful as sample transporters, mixing enhancers, dispersion eliminators and simply good discrete microreactors [3,4,5]. Aqueous droplets in microchannel are generated in a immiscible carrier fluid using T-junction or flow focusing channel [6,11]. Size of the droplets can be varied by changing the flow rates of immiscible fluids [12,13]. Reagent addition to the droplets is necessary for chemical and biological analysis. Adding a precise amount of reagents to a droplet poses difficulties and various schemes for reagent addition have been investigated by researchers.

Dosing of liquid reagents into droplets using a single T-junction in a microchannel was first demonstrated by Henkel et. al. [8]. However, those demonstrations were limited to a few flow rates of the reagents. Shestopalov et. al. [10] reported a method to adding reagents to droplets in which they injected reagents directly into the droplets. Method of injecting the reagent with the sample to form droplets at the T-junction has difficulties in precisely controlling the amount of reagents due asymmetric shear stress at the inlet boundary [14,4]. Mixing of reagents can happen in this method, before droplet formation, which interferes in the case of following instantaneous reactions and this method is not suitable for adding

different reagents and carry out subsequent reactions. Method of coalescing the droplets by surface energy pattern [16] or geometry mediation [17] has been used to force the immiscible fluid in between the individual droplets and bring into contact to coalesce them. Bremond et al. [28] proposed that decompressing emulsion droplets mechanism for the coalescence of droplets in microchannels. Use of electric [26] and electrostatic forces [18] to coalesce the droplets is not suitable for use with biological materials. Niu et al. [29] reported merging two droplets with the use of pillars in microchannels. Merging reagents into the droplets moving in the mainchannel at a T-junction (Fig. 1(a)) experience problems like synchronization of droplet arrival, contamination of the injecting stream and reliable merging only in a narrow range of flow rates [8, 3, 15]. Replacing single T-junction with multi-junction eliminates the need for synchronisation [19], but has higher fabrication cost due to the insertion of hydrophilic side channels separately. Injecting reagents alternatively from two side branches of double T-junctions increases the synchronization frequency in a wide range of flow rates but merging is not guaranteed to 100% at all flow rate conditions [21].

To overcome the above mentioned problems, we propose a design that exploits the basic fluid flow physics in the microchannel to increase the reliability of adding reagents into droplets. In this article, it will be demonstrated that an expansion in the microchannel right after the T-junction enhances the reliability in adding reagents to the preformed droplets at a T-junction.

2 Experimental details

2.1 Microchannel Design

The rational behind the provision of an expanded section lies in the answer to the following question: Why do extra droplets form? If the merging has to happen on a continuous basis

at the T-junction, droplet formation from the side channel has to be synchronized [3] with the arrival of the droplet which has already been formed and moving in the mainchannel. Otherwise an extra droplet forms, as seen in Fig. 1(a), termed as unreliable merging, a state of merging where the reagent itself forms a droplet. Garstecki et al. [11] proposed that the breakup of the two immiscible liquids at the T-junction in droplet microfluidics is dominated by the pressure built up across the droplet as it forms at low values of the capillary number ($< 10^{-2}$). Similarly, merging reagents into droplets with conventional T-junction, which has similar dynamics as that of the droplet formation at a T-junction, pressure builds up across the emerging reagent droplet due to the high resistance to the flow of continuous fluid in the thin films that separate the droplet from the walls of the microchannel, when the droplet fills almost the entire cross-section of the channel. This pressure buildup squeezes the droplet to break from the T-junction when the already formed droplet approaches it, as seen in Fig. 9(c).

Therefore, if the pressure build-up that squeezes the droplet to detach it from the T-junction can be reduced, we can avoid the extra droplet problem. We provide an expanded section, just after the T-junction, on both sides of the channel: the expansion in the side which is opposite to the droplet forming side channel provides the extra space for the carrier fluid to move forward, as seen in Fig. 1(b), so that the pressure build-up can be reduced; the expansion in the side from which the droplet forming provide the space for the droplet to grow, which allows the space for the extra volume created during the waiting time for the droplet arrival in the main channel. In doing that, there is one more additional feature added, apart from the reduced pressure drop: when the droplet breaks before merging, due to longer waiting time and droplets growing big to block the extra space, the expanded section can function like a time delay component. It can restrict the movement of the droplets and facilitate the process of droplet coalescence. Fig. 1 shows the schematic diagram of the mi-

crochannel designs (a) with conventional T-junction and (b) with an expanded section. There are three inlets to pump the fluids into the microchannel and one outlet to collect the spent fluids. The mineral oil inlet and the DI water with fluorescence inlet meet at the Y-junction and the DI water inlet from the side meet the main channel at T-junction. The expanded section is located at the distance of 50μm after the T-junction, but could be located as closely as possible, the constraint being the resolution of the photo mask. The microchannel has the height of 100 μm. The other dimensions of the microchannel are shown in Fig. 1.

2.2 Fabrication

The channel designs were printed into a photolithograhic mask and the negative SU-8 photo resist (Microchem Corp.) was used to fabricate the master mold using standard procedures specified from Microchem. Then microfluidic chips were fabricated using polydimethysiloxane (PDMS) polymer (Dow corning Sylgard 184 Silicone Elastomer) through the standard soft lithography process for PDMS microchannel fabrication [22]. The cured PDMS microchannels were bonded to another piece of flat PDMS layer after treating them with oxygen plasma. And they are allowed to recover their hydrophobicity, because of the need of the walls to be hydrophobic which facilitates the formation of water droplets in oil.

2.3 Experimental setup

The following fluids were used for the experiments: 1) Mineral oil as the carrier fluid (M5904, Sigma-Aldrich) with 2% w/w Span 80 surfactant (Sigma-Aldrich S6760), 2) DI water with fluorescent dye (0.05% w/w Acid Yellow) and 3) DI water. Hydrodynamic properties: Viscosity of DI water (μ) is 1 mPa s, interfacial tension between water and mineral oil is 3.65mNm^{-1}, contact angle between water and PDMS is 88°, viscosity of mineral oil with

2% w/w Span 80 is 23.8 mPa.s. The fluids were pumped from gas-tight syringes (Hamilton, 1.25ml) through the tubing (0.8 mm PTFE, Cole-Parmer) connected to inlets, with the help of syringe pumps (KD Scientific, Model No. 781200). The DI water with fluorescent stream forms droplets (droplet A) at the Y-junction as seen in Fig. 1. When the fluorescent droplets formed at the Y-junction reach the T-junction, the aqueous reagent stream (DI water) from the side channel is merged to the droplets. The experiments were observed under the Inverted Fluorescence Microscope (Nikon Eclipse TE2000-S) with suitable magnification using Plan Apro objectives and mercury lamp for illumination and blue filter for visualisation. The visualisation of the experiments were captured and recorded through the eye piece of the inverted microscope using a CCD camera (DCRDVD803E, SONY) and used for the analysis of the reliability of droplet merging process.

3 Testing

Experiments were carried out for the T-junction with expanded section and for the conventional T-junction designs. The combination of fluorescent stream flow rates (Q_{fluo}) and DI water flow rates (Q_{DI}) were from 0 μl/hr to 250 μl/hr in the interval of 25 μl/hr, and the mineral oil flow rate was maintained at the ratio of 1.5 to the fluorescent flow rate. Between 0 μl/hr to 25 μl/hr, intermediate flow rates of 10 μl/hr to 20 μl/hr were also used to measure the merging percentage. The flow rate ratio (FR) between mineral oil and fluorescent was kep constant at 1.5 with the aim that the droplets should be not too long or too short for this merging process. We found this ratio by changing the ratio from 0.1 to 4.0, with keeping the flow rate of fluorescence constant at 50 μl/hr. The corresponding picture is shown in Fig. 2, in which it is seen that the flow rate ratio from 1 to 2.5 produce droplet which are not too long or too short. We chose 1.5 and kept constant throughout the experiments. The videos

of the experiments were recorded for both the conventional T-junction and T-junction with expanded section designs.

4 Results and discussion

4.1 Reliability of the merging process

The recorded videos of the experiments were used to calculate the reliability of the merging process by counting the number of successfully merged droplets. The percentage of reliable merging for a particular flow rate combination was calculated as follows,

$$\%Reliability = \left(\frac{\text{number of successfully merged droplets}}{\text{total number of droplets generated for merging}} \right) \times 100. \qquad (1)$$

The contour lines indicating percent rate of droplet merging for T-junction alone and T-junction followed by an expansion of 150 μm were constructed and are shown in Figs. 3 and 4. Reliable merging (100%) for T-junction happens in a very narrow range of flow rates (below the dashed contour line) as seen in Fig. 3 and merging in a wide range of flow rate ratio gives the extra droplet problems. Microchannel with T-junction followed by an expansion provides reliable merging in a wide range of flow rates and flow rate ratio as seen in Fig. 4. The region of reliable merging is wide (region between dashed contour lines) and droplets are merged reliably in a wide range of fluorescent flow rates except at high DI water flow rates (bottom right) and low fluorescent flow rates (top-left). It is because at higher flow rates of DI water, not enough fluorescent droplets (droplet A) are formed. The low fluorescent stream cannot overcome the pressure drop of carrier fluid (mineral oil) as well the pressure drop due to high DI water flow rate to form droplets at the Y-junction. Therefore the merging percentage is low for high DI water flow rate at the top-left region in

Fig. 4. But when the flow rate becomes slightly higher, fluorescent stream can overcome the pressure drop and form enough droplets to merge reliably.

Outside the high percentage success, in general, there are three scenarios: 1) when the DI water flow rate is high and the fluorescent flow rate is low, extra droplets (droplet B) form and the merging percentage goes down; when the DI water flow rate is very high, only droplet B forms, which is not desirable as no merging is possible. 2) when the fluorescent flow rate changes from very high compared to DI water flow rate, DI water stream cannot overcome the pressure drop to merge continuously with droplet A. 3) when both fluorescent flow rate and DI water flow rate are very high, stratified flow occurs, which is not desirable for the merging process.

4.2 Droplet volumes and droplet formation time

Fig. 5 shows a sample of measurements for the volume of the droplets generated at the Y-junction for various flow rates of DI water with mineral oil flow rate fixed at the ratio of 1.5 with respect to the fluorescence flow rate for the droplet merging process. The droplet generated are consistent over time with volumes in the order of few nanolitres with less than 10% standard deviation as seen in Fig. 5. Fig. 6 shows the droplet volumes generated for various flow rates of fluorescence from the side channel at the T-junction with expansion and without expansion. These droplet volumes in the range of few nanolitres were measured from the experiments without the merging process. The volume of the droplets generated at the T-junction with expansion is higher than the volume of droplets generated at T-junction without expansion.

Fig. 7 shows the droplet formation time at the T-junction with expansion and without expansion. As expected, the droplet formation time at the T-junction with expansion is higher

than the time for the T-junction without expansion. This increase in volume and time is due to the expanded section, which reduces the pressure drop availability of extra space for droplet growth leads to longer residence time for the droplet at the T-junction.

The reliability of the merging process with an expanded section was analysed by measuring the droplet length before merging and after merging. Fig. 8 shows the droplet lengths measured before merging and after merging for different fluorescent flow rates and DI water flow rates. As we can see from Fig. 8, the length of droplets (droplet A) generated at the Y-junction (before merging) is consistent and the droplet volume decreases with the increase in the fluorescene flow rate. This also reflects in the amount of DI water merged into it at the T-junction with expansion. As the droplet length goes down, the amount of DI water merged to it also goes down because of the small residence time for the droplet the T-junction. As the DI water flow rate is increased, the amount of DI water added to the same length of droplet also goes up due to higher volume flow rate of DI water. The length of droplets after the merging process is also consistent as seen in Fig. 8.

4.3 Flow physics in the merging process

The increase in the reliability of the merging process in the T-junction with expanded section design can be explained as follows. Figure 9(a-c), shows the sequence of droplet break-up due to pressure build up at a normal T-junction. But, the expanded region right after the T-junction allows the carrier fluid to move forward avoiding the pressure build up beyond threshold-level and break-up of droplet B from the T-junction. Now, two things can happen for the droplet forming from the side channel:

1. droplet sticks to the T-junction due to surface tension and grows in the expanded region (Fig. 9(d-e)) until the droplet A merges with it (Fig. 9(f)).

2. droplet breaks away because of high droplet volume (Fig. 10(a)), due to longer waiting time for the droplet A to arrive.

In the first case, after merging, the merged droplets are squeezed from the T-junction due to pressure build up across the droplet as in the normal droplet formation process, because now the merged droplet fully occupies the channel. In the second case, droplet B and droplet A coalesce in the expanded region. The expanded region facilitates the droplets to come closer and coalesce, as seen in (Fig. 10(b)), because it acts like a time delay component and delays the forward movement of the extra-droplet in the microchannel. When the delay time is long, extra droplets occur and the merging percentage goes down. The sequence of droplet coalescence is seen in Fig. 10(a-d).

The expanded section not only eliminates the extra droplet formation but also enhances droplet merging and can be explained as follows: the extra space provided by the expanded region reduces the pressure build up that happens in the droplet formation at the T-junction and it is less than the threshold value for droplet break-up; the carrier fluid movement through the extra space exerts shear stress on the droplet forming from the side channel; therefore, the droplet formation dynamics has been changed by the expanded section at the T-junction from purely pressure dominant break-up to a combination of pressure drop and shear due to the flow of carrier fluid; the combination of shear stress and pressure buildup distorts the interface [11] and makes it flat, as seen in Fig. 9(d). The distortion remains until the fluorescent droplet (droplet A) hits the emerging DI water droplet (droplet B)(See ESI Movie1).

When the interface is flat, the curvature becomes low and the radius of curvature approaches infinity; based on the Young-Laplace equation, Laplace pressure jump ΔP_L exerted by the interface on the emerging droplet in a rectangular channel can be described

as, $\Delta P_L = \sigma\,(1/R_w + 1/R_h)$, where σ is the interfacial tension between the two phases, R_w and R_h are interface curvatures in width and height directions respectively; Laplace pressure jump, ΔP_L, across the interface is negligibly small and when the fluorescent droplet (droplet A) hits the DI water droplet (droplet B) at the T-junction, they merge easily without breaking the DI water droplet from the T-junction. Small Laplace pressure jump across the interface lowers the disturbance needed to rupture the thin film between the droplets and it reduces the possibility of droplet B breaking from the T-junction at the moment droplet A hits it. When the external pressure increases above the internal pressure at a point on the droplet surface, the droplets break up and the constituents merge.

4.4 Enhanced mixing

The merging and the coalescence patterns of droplets due to expanded section enhances mixing, because after merging the merged fluids are in axial arrangement inside the droplets as seen in Figs. 9(f) and 10(d). Tanthapanichakoon et al. [23] reported that axial arrangement of droplet constituents enhances mixing and it can be attributed to the reduction of the striation length between reactant segment by interlayering. Similar results for enhanced mixing due to axial arrangement (in-line droplet fusion) have been reported by Liu et al. and Frenz et al. [24,25]. Therefore, it can be stated that axial arrangement of droplet constituents in this merging design lead to enhanced mixing.

5 Conclusions

In conclusion, we demonstrate a design that exploits the physics of fluid flow phenomena in microchannels to eliminate the drawbacks in adding reagents into the droplets at a T-junction. An expanded section, right after the T-junction, reduces the pressure build up and

increases the residence time of the droplet at the T-junction; in the case of droplet break-up, it facilitates the coalescence of the droplets and reduces the probability of the formation of extra droplet. Holding the droplet at the T-junction leads to the distortion of the interface of the emerging droplet and becomes flat because of the shear stress and pressure buid-up due to the moving carrier fluid. A flat interface, according to the Laplace-Young equation, results in low Laplace pressure between two phases and enhances the merging of miscible droplets. Reagent addition in this design leads to axial arrangement of the droplets constituents in the merging as well as in the coalescence process and facilitates faster mixing of reactants. Therefore, the demonstrated design provides a better alternative for the available merging schemes and can be effectively used in the microfluidic chips used for biological, bio-chemical and μ-TAS assays. Effects of expansion width and length of the expanded section on the reliability of reagent addition to the droplets will be carried out in the future.

Acknowledgement. The authors gratefully acknowledge the support from the Agency of Science, Technology and Research (A*STAR), Singapore (grant number SERC 0521010108 "Droplet-based micro/nanofluidics")

References

1. Nam-Trung Nguyen and Zhigang Wu, Micromixers - a review, Journal of Micromechanics and Microengineering, 15, R1-R16 (2005).
2. Shia-Yen Teh, Robert Lin, Lung-Hsin Hung and Abraham P. Lee, Droplet microfluidics, Lab on a Chip, 8, 198-220 (2008).
3. Helen Song, DelaiL. Chen, Rustem F. Ismagilov, Reactions in droplets in microfluidic channels, Angewandte Chemie, 45, 7336-7356 (2006).
4. Bringer,M. R., Gerdts,C. J., Song,H., Tice,J. D. and Ismagilov R.F., Microfluidic systems for chemical kinetics that rely on chaotic mixing in droplets, Philosophical Transactions of the Royal Society A: Mathematical, Physical and Engineering Sciences, 362, 1087-1104 (2004).
5. Taly, V., Kelly, B. T. and Griffiths, A. D., Droplets as microreactors for high-throughput biology, ChemBioChem, 8, 263-272 (2007).
6. Stone, H. A., Stroock, A. D. and Ajdari, A., Engineering flows in small devices: Microfluidics toward a lab-on-a-chip, 36, 381-411 (2004).
7. J.M. Köhler, T. Henkel, A. Grodrian, T. Kirner, M. Roth, K. Martin, and J. Metze, Digital reaction technology by micro segmented flow-components, concepts and applications, Chemical Engineering Journal, 101, 201-216 (2004).
8. Henkel, T., Bermig, T., Kielpinski, M., Grodrian, A., Metze, J. and Köhler, J., Chip modules for generation and manipulation of fluid segments for micro serial flow processes Chemical Engineering Journal, 101, 439-445 (2004).
9. Y. Tan, J.S. Fisher, A.I. Lee, V. Cristini, and A.P. Lee, Design of microfluidic channel geometries for the control of droplet volume, chemical concentration, and sorting, Lab on a Chip, 4, 292-298 (2004).
10. Shestopalov, I., Tice, J. D. and Ismagilov, R. F., Multi-step synthesis of nanoparticles performed on millisecond time scale in a microfluidic droplet-based system Lab on a Chip - Miniaturisation for Chemistry and Biology, 4, 316-321, (2004).
11. Garstecki, P., Fuerstman, M. J., Stone, H. A. and Whitesides, G. M., Formation of droplets and bubbles in a microfluidic T-junction - Scaling and mechanism of break-up, Lab on a Chip, 6, 437-446 (2006).
12. Nisisako, T., Torii, T. and Higuchi, T., Droplet formation in a microchannel network, Lab on a Chip, 2, 24-26 (2002).
13. Christopher, G. F. and Anna, S. L., Microfluidic methods for generating continuous droplet streams, Journal of Physics D: Applied Physics, 40, R319-R336 (2007).

14. Song, H., Tice, J. D. and Ismagilov, R. F., A microfluidic system for controlling reaction networks in time, Angewandte Chemie, 42, 768-772 (2003).

15. Hatakeyama, T., Chen, D. L. and Ismagilov, R. F., Microgram-scale testing of reaction conditions in solution using nanoliter plugs in microfluidics with detection by MALDI-MS, Journal of the American Chemical Society, 128, 2518-2519 (2006).

16. Fidalgo, L. M., Abell, C. and Huck, W. T. S., Surface-induced droplet fusion in microfluidic devices, Lab on a Chip, 7, 984-986 (2007).

17. Tan, Y., Ho, Y. L. and Lee, A. P., Droplet coalescence by geometrically mediated flow in microfluidic channels, Microfluidics and Nanofluidics, 3, 495-499 (2007).

18. Sarrazin, F., Prat, L., Di Miceli, N., Cristobal, G., Link, D. R. and Weitz, D. A., Mixing characterization inside microdroplets engineered on a microcoalescer, Chemical Engineering Science, 62, 1042-1048 (2007).

19. Li, L., Boedicker, J. Q. and Ismagilov, R. F., Using a multijunction microfluidic device to inject substrate into an array of preformed plugs without cross-contamination: Comparing theory and experiments, Analytical Chemistry, 79, 2756-2761 (2007).

20. J.M. Köhler and P.A. Groß), Microphotometric characterization of fluid segment populations generated in different simple microfluidic networks, Microfluidics and Nanofluidics, 3, 653-663 (2007).

21. Um, E., Lee, D.S., Pyo, H.B. and Park, J.K., Continuous generation of hydrogel beads and encapsulation of biological materials using a microfluidic droplet-merging channel, Microfluidics and Nanofluidics, 5, 541-549 (2008).

22. M.Whitesides, G., Ostuni, E., Takayama, S., Jiang, X. and Ingber, D. E., Soft Lithography in Biology and Biochemistry, Annu. Rev. Biomed. Eng., 3, 335-373 (2001).

23. Tanthapanichakoon, W., Aoki, N., Matsuyama, K. and Mae, K., Design of mixing in microfluidic liquid slugs based on a new dimensionless number for precise reaction and mixing operations, Chemical Engineering Science, 61, 4220-4232 (2006).

24. Liu, K., Ding, H., Chen, Y. and Zhao, X.Z., Droplet-based synthetic method using microflow focusing and droplet fusion, Microfluidics and Nanofluidics, 3, 239-243 (2007).

25. Frenz, L., Harrak, A. E., Pauly, M., Bégin-Colin, S., Griffiths, A. D. and Baret, J.C., Droplet-Based Microreactors for the Synthesis of Magnetic Iron Oxide Nanoparticles, Angewandte Chemie International Edition, 47, 6817-6820 (2008).

26. Ahn, K., Agresti, J., Chong, H., Marquez, M. and Weitz, D. A., Electrocoalescence of drops synchronized by size-dependent flow in microfluidic channels, Applied Physics Letters, 88, 264105 (2006).

27. Baroud, C., de Saint Vincent, M. R. and Delville, J., An optical toolbox for total control of droplet microfluidics, Lab on a Chip, 7, 1029-1033 (2007).

28. Bremond, N., Thiam, A. R. and Bibette, J., Decompressing Emulsion Droplets Favors Coalescence, Physical Review Letters, 100, 024501 (2008).

29. Niu, X., Gulati, S., Edel, J. B. and deMello, A. J., Pillar-induced droplet merging in microfluidic circuits, Lab on a Chip, 8, 1837-1841 (2008).

30. März, A., Ackermann, K. R., Malsch, D., Bocklitz, T., Henkel, T. and Popp, J., Towards a quantitative SERS approach - online monitoring of analytes in a microfluidic system with isotope-edited internal standards, Journal of Biophotonics, 4, 232-242 (2009).

Captions of figures

Fig. 1 Schematic of the droplet merging channel with expansion. ΔP_{in} is the interfacial pressure difference between the oil and DI water

Fig. 2 Length of droplets vs flow rate ratios of mineral oil and fluorescence

Fig. 3 Critical volume of the droplets formed at the Y-junction

Fig. 4 Critical volume of the droplets formed at the conventional T-junction and T-junction with expansion

Fig. 5 Time for droplet formation at the conventional T-junction and T-junction with expansion

Fig. 6 Contour plot for merging of reagents into droplets with conventional T-junction

Fig. 7 Contour plot for merging with T-junction and subsequent expansion

Fig. 8 Droplet merging phenomena in: (a-c) - extra droplet formation in a conventional T-junction, (d-f) -merging of droplets before break off in a T-junction followed by an expanded section

Fig. 9 Coalescence of droplets in the expanded section after droplet break-up

Fig. 10 Droplet lengths before merging and after merging for various flow rates of fluorescence and DI water

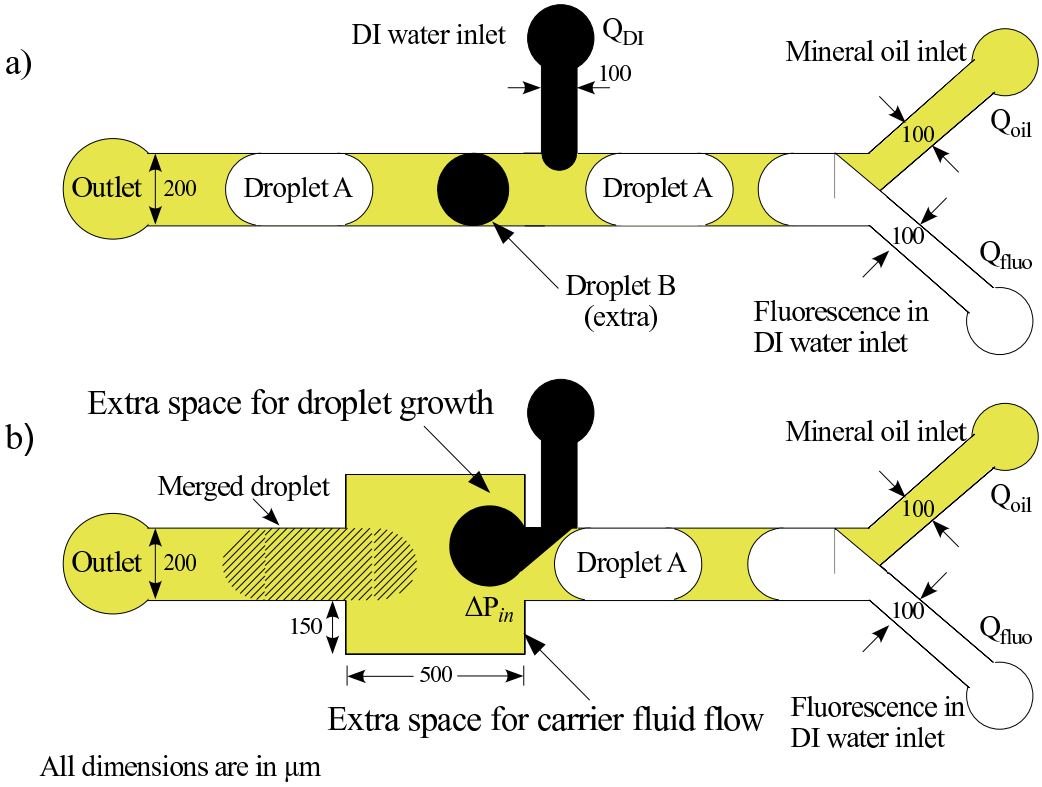

Fig. 1 Schematic of the droplet merging channel: a) conventional T-junction b) T-junction with expansion. ΔP_{in} is the interfacial pressure difference between the oil and DI water

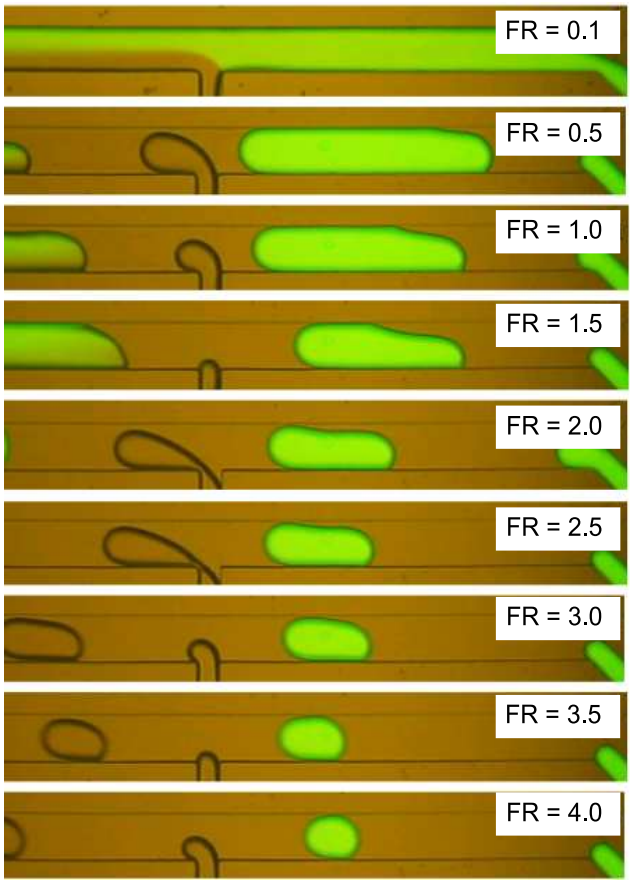

Fig. 2 Droplet length vs flow rate ratios of mineral oil and fluorescence

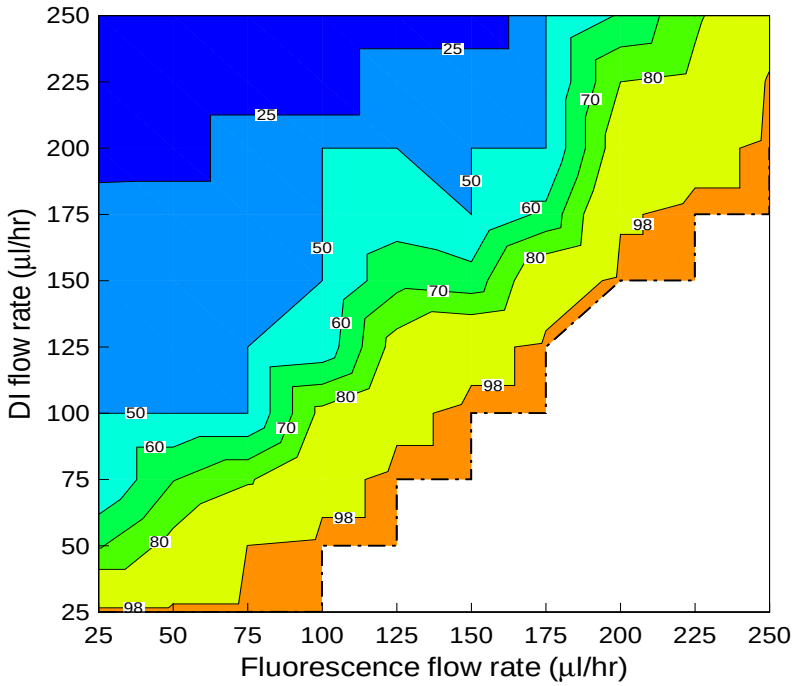

Fig. 3 Contour plot for merging of reagents into droplets with conventional T-junction

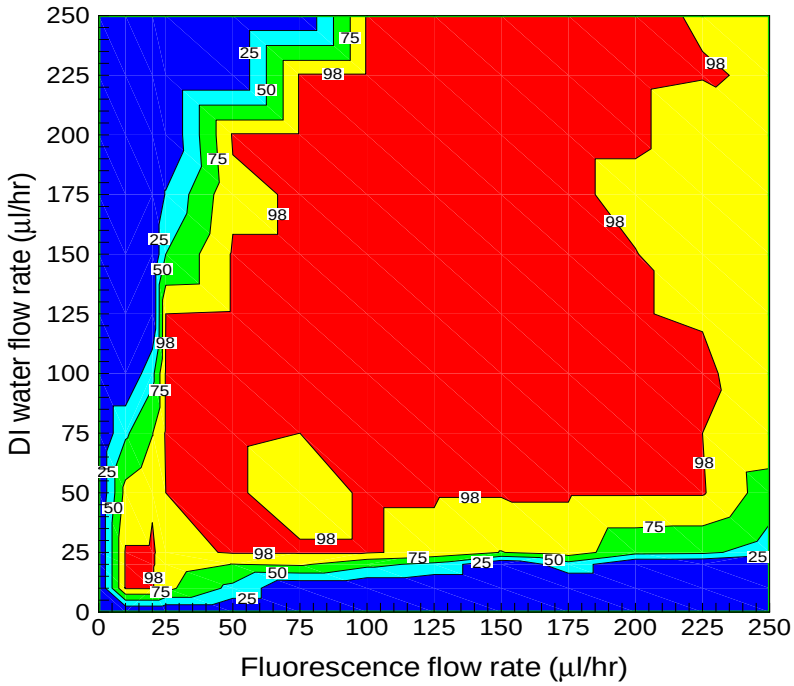

Fig. 4 Contour plot for merging with T-junction and subsequent expansion

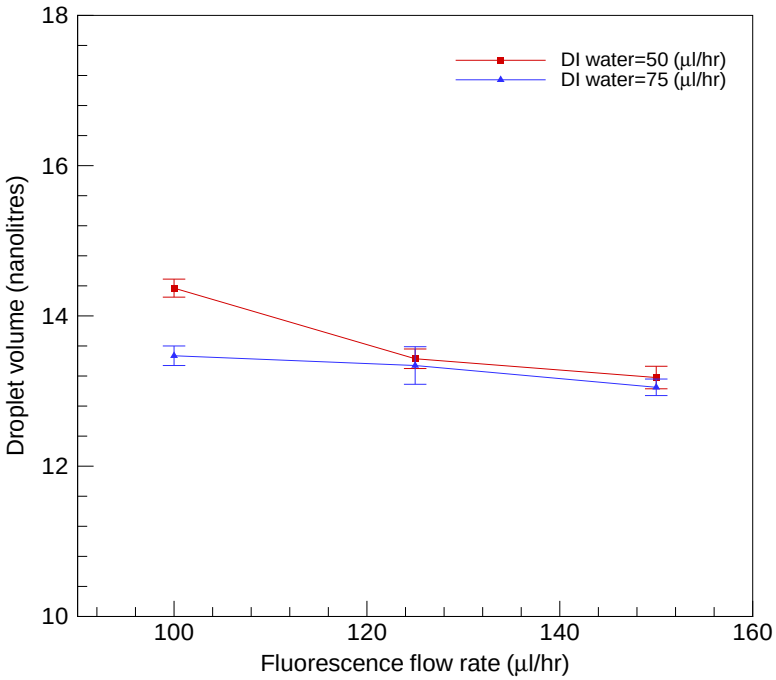

Fig. 5 Volume of the droplets formed at the Y-junction

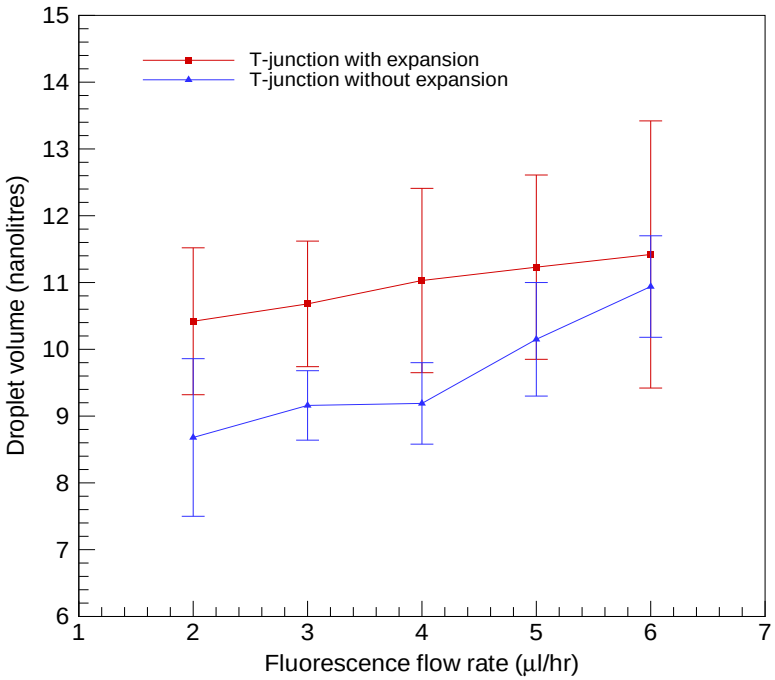

Fig. 6 Critical volume of the droplets formed at the conventional T-junction and T-junction with expansion

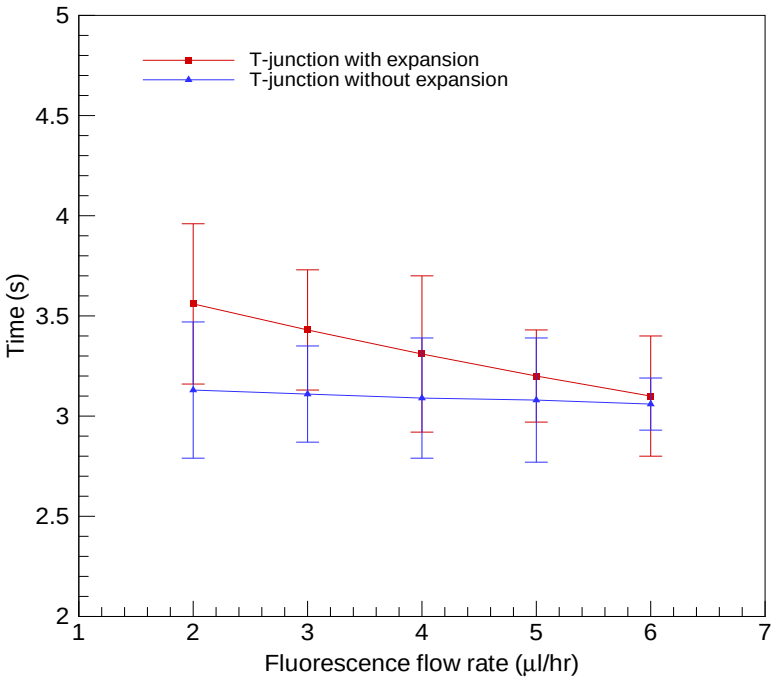

Fig. 7 Time for droplet formation at the conventional T-junction and T-junction with expansion

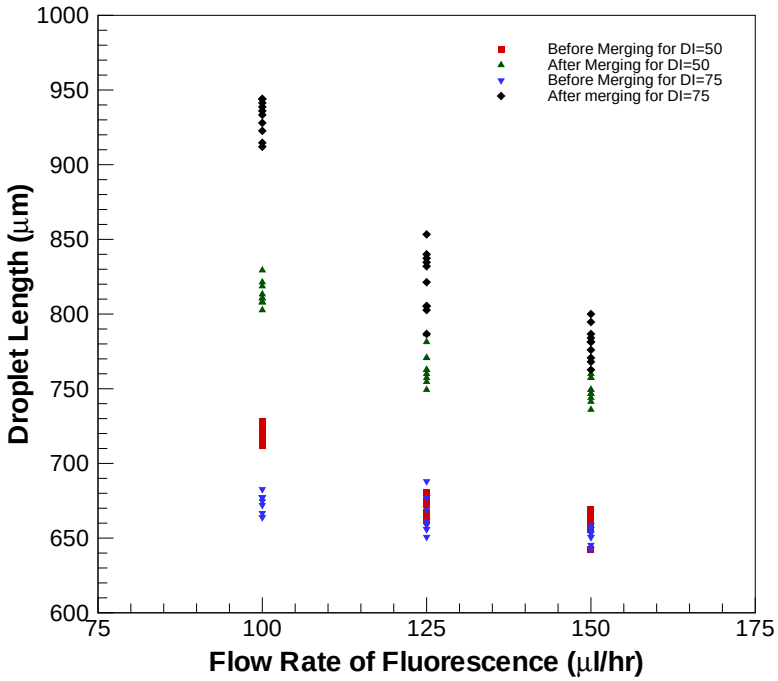

Fig. 8 Droplet lengths before merging and after merging for various flow rates of fluorescence and DI water

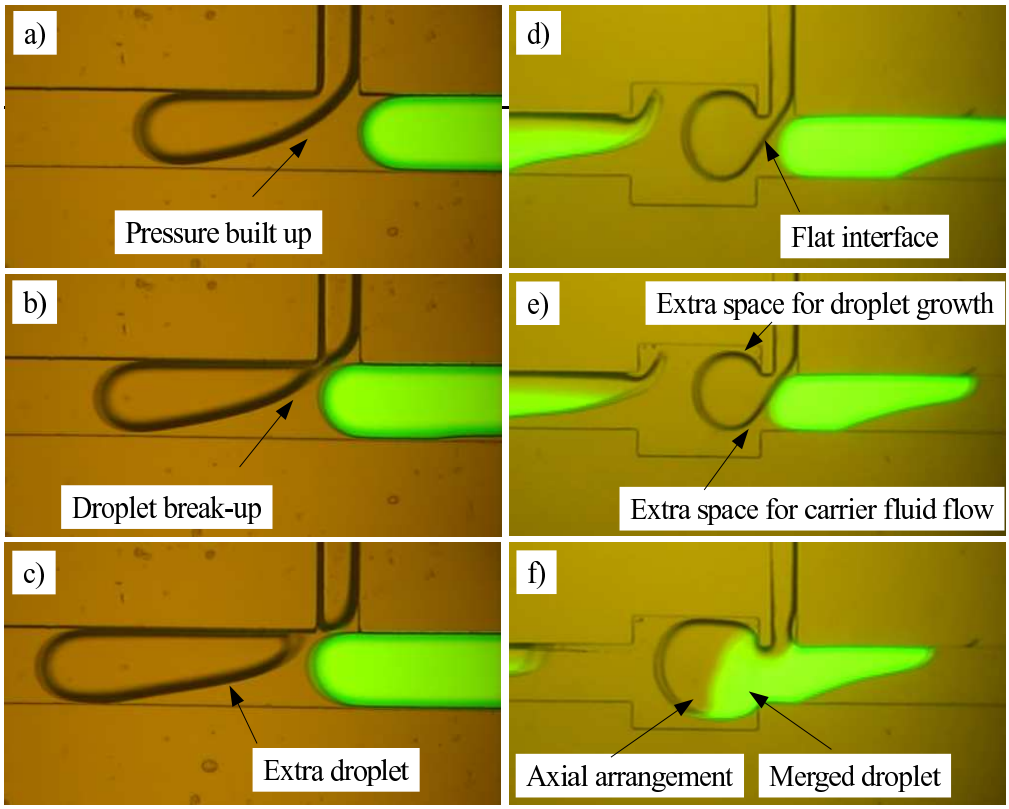

Fig. 9 Droplet merging phenomena in: (a-c) - extra droplet formation in a conventional T-junction, (d-f) - merging of droplets before break off in a T-junction followed by an expanded section

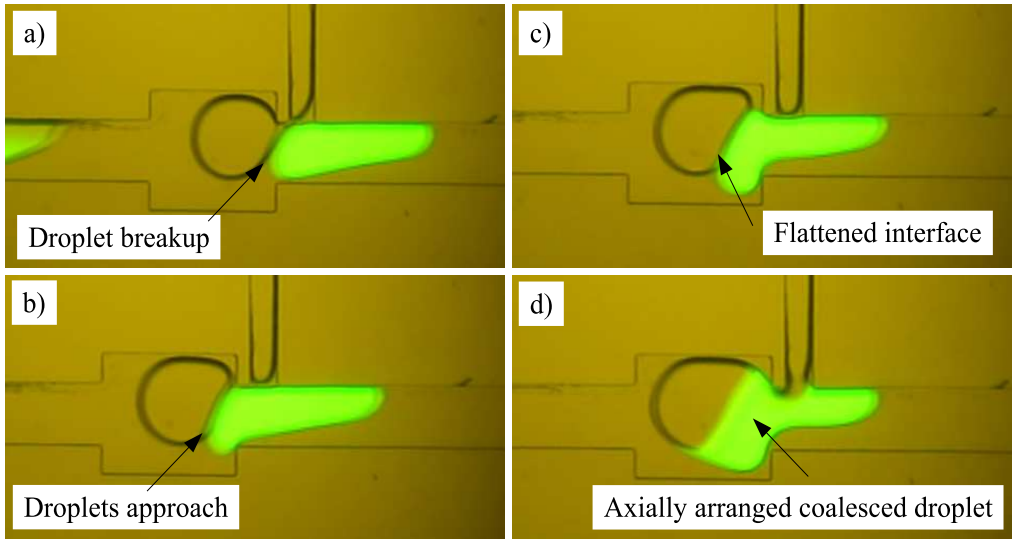

Fig. 10 Coalescence of droplets in the expanded section after droplet break-up